Future perspective of polymer solar cells based on recent in-depth understanding of photovoltaic conversion mechanism

AUTHOR(S):

Ohkita, Hideo

JSAP Review
JSAP Rev. **2022**, 220207
https://doi.org/10.11470/jsaprev.220207

Tutorial Review

Future perspective of polymer solar cells based on recent in-depth understanding of photovoltaic conversion mechanism

Hideo Ohkita

Department of Polymer Chemistry, Graduate School of Engineering, Kyoto University, Kyoto 615-8510, Japan
E-mail: ohkita@photo.polym.kyoto-u.ac.jp

In this review, I will discuss the improvement of photovoltaic parameters, such as short-circuit current density (J_{SC}), open-circuit voltage (V_{OC}), and fill factor (FF), in terms of photophysical elementary processes of photovoltaic conversion in polymer solar cells. These elementary processes can be directly observed using time-resolved spectroscopic measurements. Thus, I will introduce the latest research topics, focusing on these spectroscopic analyses. Finally, I will mention future prospects for further improvements in the power conversion efficiency of polymer solar cells.

Received June 24, 2022; Accepted July 25, 2022
Translated from Oyo Buturi **91**, 668 (2022) DOI: https://doi.org/10.11470/oubutsu.91.11_668

1. Preface

Polymer solar cells are composed of organic semiconductors, such as conjugated polymers and conjugated low-molecular-weight organic semiconductors, in the photoactive layer. Hence, they have several advantages in terms of physical properties such as lightweight and flexibility, and also can be produced via the printing techniques based on solution processes. Therefore, polymer solar cells have been widely studied and developed as next-generation solar cells in the world. In 1995, Friend and Heeger et al. independently published pioneering papers on polymer solar cells using conjugated polymers, although the power conversion efficiency (PCE) was less than 1% [1,2]. Friend et al. reported polymer solar cells using electron-donating conjugated polymers and electron-accepting conjugated polymers. Heeger et al. reported polymer solar cells using electron-donating conjugated polymers and electron-accepting fullerene molecules. In both cases, the efficiency was dramatically improved by using a blend film in which a donor material and an acceptor material are mixed as a photoactive layer. Such a blend structure was called an interpenetrating polymer network by Friend et al. and a bulk heterojunction (BHJ) by Heeger et al. Since then, polymer solar cells composed of conjugated polymers and fullerenes have been mainly studied, and the name bulk heterojunction is widely used up to now. In 1991, before the publication of the two papers, Hiramoto et al. already reported that the PCE can be improved by mixing donor and acceptor materials in a low-molecular-weight organic thin-film solar cell [3]. This donor/acceptor mixed structure is a breakthrough approach and still the basic structure of organic thin-film solar cells. After this breakthrough, the PCE has been steadily improved with the development of new materials, largely owing to the diversity of organic materials. Typical examples include the highly soluble fullerene PCBM with substituents [4], crystalline conjugated polymer P3HT [5], low-bandgap conjugated polymer PTB7 [6], which is an alternating copolymer of donor and acceptor units, and nonfullerene acceptor molecule ITIC [7]. Another breakthrough in device structure following the BHJ structure is a ternary blend device that introduces a third component in addition to the donor and acceptor materials. This makes it possible to overcome the limitation of the narrow absorption band of organic semiconductors and to expand the light-harvesting band simply and effectively. In 2009, we demonstrated that the short-circuit current density (J_{SC}) was effectively improved by addition of the phthalocyanine near-infrared dye SiPc into a P3HT/PCBM binary device [8]. Very recently, a ternary blend device using a conjugated polymer and nonfullerene acceptor has been reported with a certified efficiency of 19.2% [9]. Efficiencies over 20% will be achieved in the near future.

As mentioned above, the efficiency improvement of polymer solar cells is largely due to the invention of new device structures, such as the BHJ structure and the ternary blend structure, as well as the development of new materials. Simultaneously, fundamental research on the photovoltaic conversion mechanism has contributed considerably to the efficiency improvement. This is because a deeper understanding of the photovoltaic conversion mechanism has enabled more rational material design and more effective development of highly efficient new materials. In this paper, we describe analytical approaches to the J_{SC}, open-circuit voltage (V_{OC}), and fill factor (FF) of polymer solar cells in terms of photophysical elementary processes in photovoltaic conversion and discuss strategies for further improving these photovoltaic parameters.

2. Photophysical elementary process of photovoltaic conversion in polymer solar cells

As mentioned before, the photoactive layer of a polymer solar cell generally has a blend structure of a donor material and an acceptor material. However, here, for simplicity, we consider a bilayered film structure of a donor material and an acceptor material (Fig. 1(a)). When such a bilayer film is irradiated with sunlight, the light is absorbed by the donor or acceptor material, and excitons are generated. Here, the case where the light is absorbed by the donor material is illustrated. Excitons generated in organic semiconductors are mostly Frenkel excitons localized to molecular size. As the dielectric constant of organic materials is only approximately 3 at most, the electrons and holes in the excitons are strongly bound by the Coulomb attraction and cannot be dissociated at an energy of approximately k_BT at room temperature. In contrast, the excitons generated in inorganic semiconductors are Wannier excitons spread in the crystal,

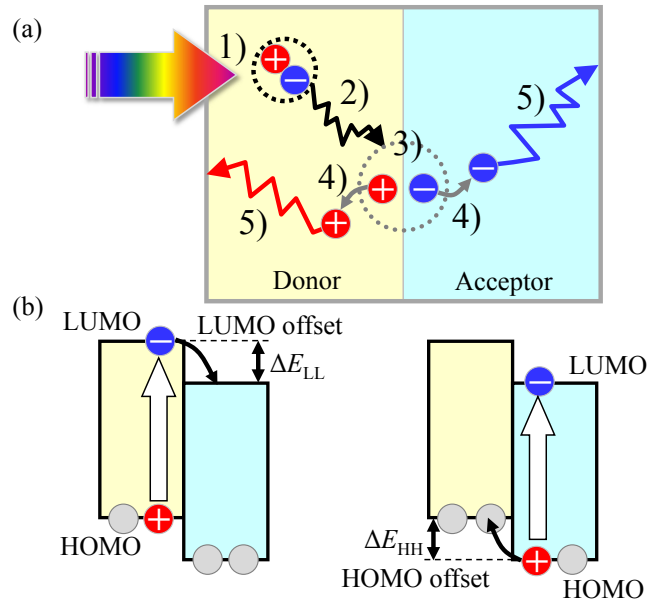

Fig. 1. (a) Photophysical elementary processes of photovoltaic conversion in polymer solar cells: 1) photon absorption, 2) exciton diffusion, 3) charge transfer, 4) charge dissociation, 5) charge collection. (b) Relationship between HOMO and LUMO energy levels for donor (yellow) and acceptor (light blue) materials: (Left) Charge transfer by LUMO offset ΔE_{LL} upon donor excitation. (Right) Charge transfer by HOMO offset ΔE_{HH} upon acceptor excitation.

and partly because of their high dielectric constant, they can easily dissociate into charge carriers even at room temperature. Therefore, the driving force to dissociate excitons into electrons and holes is required to generate charge carriers in polymer solar cells. This is a decisive difference from the charge generation mechanism in inorganic solar cells. Excitons generated in organic semiconductors cannot spontaneously dissociate into charge carriers but can diffuse in the film as excitons consisting of electron–hole pairs. However, as an exciton has a lifetime of approximately 1 ns, it can diffuse only approximately 10 nm. Therefore, in the bilayer film shown in Fig. 1(a), some excitons cannot reach the interface, and hence cannot dissociate into charge carriers. Therefore, the BHJ structure described above is essential for efficient charge generation. When excitons generated in the donor material reach the heterojunction interface with the acceptor material, electrons are transferred to the acceptor material, leaving holes in the donor material, and generating charge carriers. This is because the LUMO level of the donor material is higher in energy than the LUMO level of the acceptor material, as shown in Fig. 1(b). Therefore, it is believed that donor excitons can be converted into electrons of the acceptor material and holes of the donor material using this energy difference as a driving force. When excitons are generated in the acceptor material, the driving force is the HOMO level difference at the heterojunction interface. The electrons and holes generated at the heterojunction interface thus can be regarded as charge transfer (CT) states; hence, they are also called CT excitons. When the CT exciton state is released from Coulomb binding and dissociates into electron and hole charge carriers, the electron carriers are transported in the acceptor material and the hole carriers are transported in the donor material to the anode and cathode, respectively, and finally photocurrent is generated. Therefore, the series of photophysical elementary processes described above can be classified into the following five steps: 1) exciton generation by light absorption, 2) exciton diffusion to the heterojunction interface, 3) charge transfer at the heterojunction interface, 4) charge dissociation from CT excitons to charge carriers, and 5) charge collection to each electrode. Therefore, all the photophysical elementary processes must proceed with high efficiency to generate photocurrent efficiently.

3. Analysis of device properties

3.1 Short-circuit current density

As mentioned above, the short-circuit current density (J_{SC}) is proportional to the product of efficiencies in the five photophysical elementary processes: light absorption efficiency (η_A), exciton diffusion efficiency (η_{ED}), charge transfer efficiency (η_{CT}), charge dissociation efficiency (η_{CD}), and charge collection efficiency (η_{CC}). The product of these efficiencies at each wavelength of illuminating light is equal to the external quantum efficiency (EQE) of the solar cell device at that wavelength. Therefore, if it is possible to evaluate each of these efficiencies, it will be possible to clarify the limiting process in J_{SC}. The time scales of these five photophysical elementary processes in photovoltaic conversion are as follows: the time required for light absorption is on the order of 10^{-15} s, which is an electronic transition; the time required for exciton diffusion to the heterojunction interface is approximately 10^{-13}–10^{-10} s, depending on the domain size; the time required for the generation of CT excitons at the interface to compete for dissociation to charge carriers with geminate recombination is approximately 10^{-9} s; and the time required for the charge carriers to be collected at the electrode is approximately 10^{-7}–10^{-6} s. In other words, to observe all the elementary processes from the light absorption to the charge collection at the electrode, a measurement technique that can track transient events on a time scale of 10^{-15}–10^{-6} s is required.

Time-resolved spectroscopy using a short-pulse laser is the most suitable measurement method for tracking such transient events directly. We have studied the charge generation dynamics in various polymer solar cells using laser spectroscopy [10–13]. Here, as an example, the results of the transient absorption measurement of P3HT/PCBM blend films are taken to explain how to evaluate the charge dissociation efficiency (η_{CD}) [14]. The broken line in Fig. 2 is

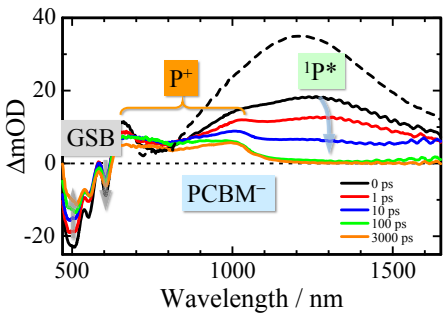

Fig. 2. Transient absorption spectra of RR-P3HT/PCBM blend films: P3HT singlet exciton ($^1P^*$), P3HT polaron (P^+), PCBM anion ($PCBM^-$), and ground state bleaching (GSB). Broken line represents transient absorption spectrum of RR-P3HT neat films at 0 ps.

the transient absorption spectrum of the P3HT neat film, which can be attributed to the absorption of singlet excitons in P3HT. The solid lines are the transient absorption spectra of the blend film, which show that half of singlet excitons already decayed immediately after excitation (0 ps). Simultaneously, new absorption bands attributed to P3HT polarons were observed at around 700 nm and 1000 nm, indicating that charges were generated immediately after the excitation. The time evolution of each transient component obtained by spectral analysis shows that the singlet exciton decays with a time constant of approximately 10 ps, and the P3HT polaron is generated with the same time constant. In other words, the charge is generated from the singlet exciton. Focusing on the spectra after 100 ps, singlet excitons have almost disappeared and instead a negative signal attributed to ground-state photobleaching (GSB) is observed at around 500–600 nm. This GSB is due to the decrease in the ground state caused by the generation of excitons and charge carriers. In this case, it is attributed to the generation of charge carriers, because no excitons are observed during this time period. Interestingly, the GSB decreased (recovered) in the short-wavelength region at around 500 nm but increased in the long-wavelength region at around 600 nm. The ground-state absorption of P3HT, which is a crystalline polymer, is attributed to the amorphous phase in the short-wavelength region and the crystalline phase in the long-wavelength region. Therefore, the time evolution of the GSB indicates that the P3HT polarons in the amorphous phase undergo hole transfer to the crystalline phase. Blend films using crystalline conjugated polymers, such as P3HT, and highly aggregated molecules, such as PCBM, consist of three phases: the crystalline phase of P3HT, the aggregated phase of PCBM, and the mixed phase of P3HT and PCBM. The mixed-phase P3HT is mixed with PCBM in an amorphous state, and has a shorter effective conjugation length and a deeper HOMO level than the crystalline P3HT. Similarly, PCBM dispersed in the mixed phase has a shallower LUMO level than PCBM in the aggregated phase. Therefore, at the heterojunction interface of the P3HT/PCBM blend film, both the HOMO and LUMO levels are considered to form a cascade of energy levels. The hole transfer from the amorphous phase to the crystalline phase of the P3HT polaron described above indicates the hole transfer from the mixed phase to the crystalline phase.

We can discuss the decay mechanism of the generated charges by measuring the dynamics of such charge carriers under different excitation light intensities. For example, when the generated electron–hole pairs recombine geminately without dissociating into free charge carriers, the lifetime is independent of the excitation light intensity (initial concentration) because it is a first-order reaction. In contrast, when the generated electron–hole pairs dissociate into free charge carriers and undergo bimolecular recombination with other charge carriers, the lifetime depends on the excitation light intensity (initial concentration) because it is a second-order reaction. In this case, the lifetime (half-life) becomes shorter as the excitation intensity increases (higher initial concentration). Considering the P3HT/PCBM blend as an example, in RRa-P3HT/PCBM using amorphous regiorandom P3HT (RRa-P3HT), the decay of the P3HT polaron does not depend on the excitation light intensity and is dominated by geminate recombination. In RR-P3HT/PCBM using crystalline regioregular P3HT (RR-P3HT), the decay of the P3HT polaron depends on the excitation light intensity, indicating that bimolecular recombination is dominant. Under low-intensity excitation conditions, such as sunlight, the initial bimolecular recombination is negligible, whereas geminate recombination proceeds regardless of the intensity. Therefore, the charge dissociation efficiency (η_{CD}) can be evaluated by analyzing the percentage of long-lived charges under weakly excited conditions.

Table 1. Photovoltaic conversion efficiencies in various polymer solar cells.

Polymers	Morphology	η_{ED}	η_{CD}	ΔE_{LL} / eV	Refs
PNOz4T	Highly crystalline	~0.6	~1	~0.1	15
RR-P3HT annealed	Highly crystalline	~0.9	>0.9	~1.1	14,16,17
RR-P3HT as cast	Crystalline	~0.95	~0.8	~1.1	14,18
PNTz4T	Crystalline	>0.95	~0.75	~0.3	15,19
PSBTBT	Slightly crystalline	~1	~0.75	~0.4	20,21,22
PCPDTBT (w DIO)	Slightly ordered	~1	~0.7	~0.3	23
PCPDTBT (w/o DIO)	Negligibly ordered	~1	~0.5	~0.3	23
N-P7	Amorphous	~1	~0.65	~0.4	24
RRa-P3HT	Amorphous	~1	~0.3	~1.2	14

Table 1 summarizes the results of similar analyses for other systems. Here, as the charge transfer efficiency (η_{CT}) can be assumed to be 1 for a system with a sufficient energy offset, the exciton diffusion efficiency (η_{ED}) is evaluated by the photoluminescence quenching efficiency Φ_q ($= \eta_{ED}\eta_{CT}$) obtained from the emission intensity in neat and blend films. In Table 1, blend films using conjugated polymers with higher crystallinity are shown listed in upper lines. As shown in the table, η_{ED} tends to decrease as the crystallinity increases. This is because the higher the crystallinity of the conjugated polymer, the larger is the crystal domain formed, and hence some of the excitons generated in the domain cannot reach the interface. In contrast, η_{CD} tends to increase as the crystallinity increases. For conjugated polymers with low crystallinity, η_{CD} is improved by increasing PCBM aggregates by forming a film from a solution containing additives, such as diiodooctane. Thus, the high crystallinity of the polymer and the aggregation of PCBM are important factors for realizing highly efficient charge dissociation. Interestingly, as shown in the table, η_{CD} is almost unity in the PNOz4T/$PC_{71}BM$ blend film, which is a highly crystalline conjugated polymer [15]. Although the LUMO offset ΔE_{LL} is very small, less than 0.1 eV, this system gives a high charge dissociation efficiency. As mentioned in the previous section, in organic thin-film solar cells, an energy offset of approximately 0.3 eV is believed to be required at the heterojunction interface as a driving force to break the Coulomb attraction to dissociate excitons into charge carriers. Therefore, this result indicates that large energy offset is not always necessary to realize highly efficient charge generation, suggesting that more efficient polymer solar cells can be realized with smaller energy losses. Mechanisms explaining highly efficient charge dissociation, such as high local mobility [25], charge generation from hot excitons [26,27], charge generation from

relaxed excitons [28], charge delocalization [14,29,30], entropy effects [31,32], and cascade structures [14,33,34], have been proposed. Although the entropy effect is expected to show temperature dependence, no temperature dependence for efficient polymer solar cells. Hence, a model that introduces energy disorder in addition to the entropy effect [35] and a model that considers the nonequilibrium state [36] have been proposed. Regarding the cascade structure, it has been pointed out that nonfullerene acceptors may form an energy gradient at the heterojunction interface owing to the quadrupole effect [37]. Thus, a deeper understanding of the mechanism of highly efficient charge dissociation is required to achieve even higher efficiency.

3.2 Open-circuit voltage

The open-circuit voltage (V_{OC}) is the potential difference corresponding to the quasi-Fermi energy difference between the electrons and holes generated in the solar cell. In inorganic semiconductors, electrons exist in the conduction band and holes in the valence band. Therefore, the upper limit of V_{OC} is the bandgap energy E_g, which is the energy difference between the conduction and valence bands. In practice, only a reduced voltage is obtained because of recombination losses. In polymer solar cells, hole carriers are located at the HOMO level of the donor material and electron carriers at the LUMO level of the acceptor material. Thus, the potential energy difference between the HOMO level of the donor material and the LUMO level of the acceptor material is the upper limit of V_{OC}. In other words, the LUMO offset ΔE_{LL} and the HOMO offset ΔE_{HH} are inevitably lost from the bandgap energy E_g of each material. In polymer solar cells, there is an additional absorption band owing to the CT state below the E_g of the low-energy absorption band among the materials, which is different from the inorganic semiconductor solar cell. To understand this difference, we use a modified Shockley–Queisser (SQ) model [38–42] to discuss the loss mechanism specific to organic thin-film solar cells.

In solar cells, there are two types of recombination losses: radiative recombination loss and nonradiative recombination loss. The former is the reverse process of light absorption; hence, it cannot be avoided in solar cells. First, let us consider the radiation recombination loss. In the SQ model, a rectangular spectrum is assumed: the absorptance $\alpha(E)$ of the photoactive layer with respect to light energy E is 0 below E_g and 1 above E_g. On the other hand, considering a modified SQ model using a two-step spectrum, it is assumed that the $\alpha(E)$ is 0 below E_{CT}, is α_{CT} between E_{CT} and E_g, and is 1 above E_g (Fig. 3(a)). In this case, the radiative recombination loss from the E_g is given by the following equation. For details, please refer to the previous report [42].

$$qV_{OC} = E_g - \Delta qV_{r1} - \Delta qV_{r2} - \Delta qV_{SC}, \quad (1)$$

where q is the elementary charge, ΔqV_{r1} is the radiative recombination loss owing to the absorption band above E_g, ΔqV_{r2} is the radiative recombination loss owing to the absorption band between E_{CT} and E_g, and ΔqV_{SC} represents the voltage loss caused by the current loss owing to the deviation of the absorption spectrum from the rectangular shape. In the SQ model, $\Delta qV_{r2} = \Delta qV_{SC} = 0$ and the loss term is ΔqV_{r1} only. In contrast, in the modified SQ model, ΔqV_{r2} and ΔqV_{SC} are added as new loss terms. As an example, Fig. 3(b) shows the change in these loss terms with respect to E_{CT} under the conditions of $E_g = 1.5$ eV and $\alpha_{CT} = 10^{-4}$. Among them, ΔqV_{SC} is less than 0.01 eV, which is negligibly small compared with the other terms. As ΔqV_{r1} is dependent upon E_g, it takes a constant value regardless of E_{CT} under the same E_g. On the other hand, ΔqV_{r2} increases as E_{CT} decreases under the same E_g (an E_g of 1.5 eV in Fig. 3(b)). This indicates that the more clearly the CT absorption band is observed below E_g, the more the additional radiation loss component specific to organic thin-film solar cells increases.

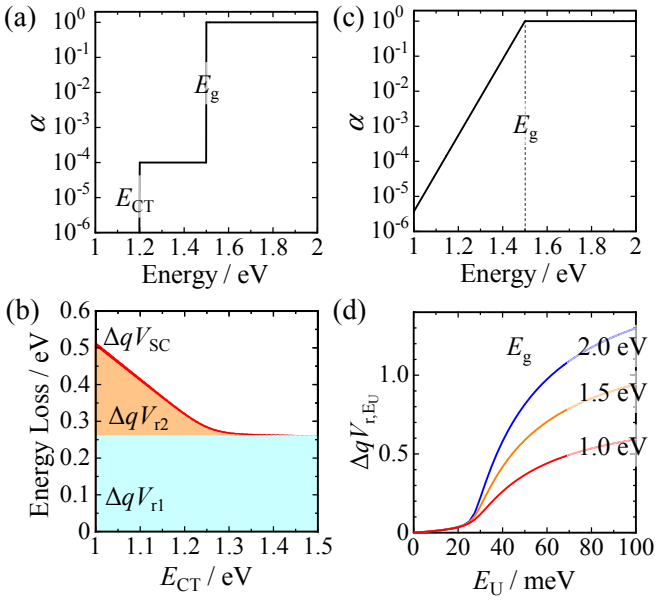

Fig. 3. (a) Two-step rectangle absorption spectrum based on exciton and CT bands: E_g =1.5 eV, E_{CT} =1.2 eV, $\alpha_{CT} = 10^{-4}$. (b) Each energy loss plotted against E_{CT}: ΔqV_{r1} is the radiative recombination loss due to the exciton band above E_g (light blue), ΔqV_{r2} is the radiative recombination loss due to the CT band between E_{CT} and E_g (orange), ΔqV_{SC} is the energy loss due to current loss (red). (c) Absorption spectrum based on rectangle exciton band and Urbach tail band (E_U = 40 meV). (d) Radiative recombination loss due to the Urbach tail $\Delta qV_{r,Eu}$ plotted against E_U. Adapted from Ref. 42 with permission from the Royal Society of Chemistry.

We next consider a modified SQ model in which an exponential Urbach absorption tail, instead of the rectangular CT absorption band, exists in the region below E_g (Fig. 3(c)). On the basis of this model, the radiation loss $\Delta qV_{r,Eu}$ owing to the Urbach absorption tail is as small as 0.05 eV or less if the Urbach energy E_U is less than k_BT (~25 meV); however, above this value, it increases significantly (Fig. 3(d)). In inorganic semiconductors, such as crystalline silicon (c-Si) and GaAs, E_U has a small value of approximately 10 meV, whereas the corresponding value for organic semiconductors is approximately 30–60 meV, which is much larger than k_BT [43]. In most of organic thin-film solar cells, therefore, the radiation loss owing to the effect of the absorption edge below E_g cannot be ignored even in systems where the CT absorption band is almost absent. Recently, on the other hand, polymer solar cells using highly crystalline conjugated polymers or nonfullerene acceptors, which are fused-ring π-conjugated molecules, show small values of E_U of the order of 20 meV, and the radiation loss is considerably suppressed.

In addition to the radiative recombination loss described above, nonradiative recombination loss is involved in an

actual device. In polymer solar cells, the CT state is the recombination center, in which the radiative transition intensity of the CT state is much smaller than that of the exciton absorption band. Thus, the nonradiative recombination loss is the dominant loss channel. The nonradiative loss energy ΔqV_{nr} can be evaluated using Eq. (2) by measuring the electroluminescence quantum yield EQE_{EL} of the device.

$$\Delta qV_{nr} = -k_B T \ln(EQE_{EL}) \tag{2}$$

In conventional conjugated polymer/fullerene blends, EQE_{EL} values are extremely low, on the order of 10^{-8}, and ΔqV_{nr} values exceeding 0.4 eV have been reported. In contrast, polymer solar cells using highly crystalline conjugated polymers or nonfullerene acceptors, which are fused-ring π-conjugated molecules, have EQE_{EL} values of the order of 10^{-4} and ΔqV_{nr} values of 0.2–0.3 eV [44]. In particular, polymer solar cells using nonfullerene acceptors as low-bandgap materials have been reported to exhibit ΔqV_{nr} values of 0.2 eV or less [45]. These systems are characterized by a small ΔE_{HH} and close proximity between the exciton level of the luminescent nonfullerene acceptor and the CT level. The radiative transition intensity from the CT level is enhanced by borrowing the radiative transition intensity of nonfullerene acceptor excitons [46]. Thus, further improvement of V_{OC} requires materials with as small an offset as possible so that the CT absorption band is not observed, highly ordered materials to reduce E_U as much as possible, and the development of materials with high photoluminescence efficiency to achieve a high EQE_{EL}value.

3.3 Fill factor

The fill factor (FF) is a device parameter that is less intuitive than J_{SC} and V_{OC}; it indicates how efficiently charge carriers are collected in comparison with charge recombination. Recently, it has been reported that θ, given by Eq. (3), which corresponds to the ratio of the charge recombination rate to the charge collection rate, shows a good correlation with the FF [47]. In other words, the smaller θ is, the faster the charge collection is compared with the recombination, and the less is the charge collection loss.

$$\theta = \frac{\gamma G L^4}{\mu_n \mu_p V_{int}^2}, \tag{3}$$

where γ is the bimolecular recombination rate, G is the charge generation rate per unit volume, L is the thickness of the active layer, μ_n and μ_p are the electron and hole mobilities, respectively, and V_{int} is the internal voltage in the device. The α, which is given by Eq. (4), has been proposed as a further improved index of θ, and it has been reported that, for $\alpha < 1$, the device exhibits the same FF dependence as the Shockley diode model [48].

$$\alpha^2 = \left(\frac{qV_{int}}{2k_B T}\right)^2 \theta \tag{4}$$

In most organic thin-film solar cells, $\alpha > 1$, which has been indicated as a transport-limiting case.

As the FF is limited by the charge transport in several systems as described above, recombination kinetics parameters under light irradiation conditions can be evaluated and used to reproduce the J–V curve [49].

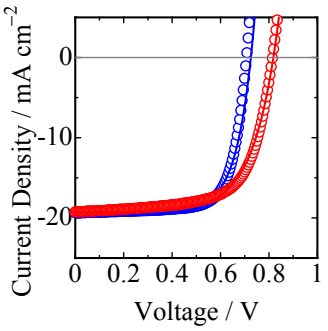

Fig. 4. J–V characteristics measured (circles) and reproduced with recombination kinetic parameters (solid line) under simulated solar illumination: PNTz4T/PC_{70}BM (blue), PNTz4TF2/PC_{70}BM (red). Adapted from Ref. 19 with permission from the American Chemical Society.

$$J = J_{gen} + J_{loss}(V)t = J_{gen} - \frac{qL\,n(V)}{\tau(V)} \tag{5}$$

The recombination current $J_{loss}(V)$ can be obtained by evaluating the charge carrier density $n(V)$ and lifetime $\tau(V)$ through transient photovoltage/photocurrent measurements and charge extraction measurements. In addition, when the charge generation current J_{gen} does not depend on the bias, the value can be approximated as $J_{gen} \approx J_{SC}$. Figure 4 shows an example of reproducing the J–V curve using the recombination kinetic parameters obtained through the above analysis [19]. Except for the presence or absence of fluorine substituents, the devices based on PNTz4F and PNTz4TF2, which are crystalline conjugated polymers with the same main chain backbone, blended with PC_{71}BM show almost the same J_{SC}, but there are differences in V_{OC} and FF. As shown in the figure, the J–V curve can be reproduced using the recombination kinetic parameters for all the devices. Thus, the FF is dominated by charge recombination dynamics. In fact, the index α in this system is greater than 1, corresponding to transport-limiting. If the J–V curve cannot be reproduced by the above analysis, other factors may be involved. For example, if the J–V curve cannot be reproduced assuming a constant J_{gen}, the charge generation current $J_{gen}(V)$ may be bias dependent [50]. In addition, when isolated domains exist, the charge collection measurement may underestimate the charge density, and the J–V curve cannot be reproduced. In such a case, conversely, the concentration of isolated charge carriers can also be estimated from the difference between the measured and reproduced values.

Recently, an FF exceeding 0.8 has been reported for efficient polymer solar cells [51]. As θ of the order of 10^{-4} has been reported for this device, it corresponds to $\alpha < 1$ when converted to α, suggesting that the device corresponds to the Shockley diode model. In fact, this value shows good agreement with the FF empirical formula based on the equivalent circuit model for the Shockley diode. These reports indicate that polymer solar cells can be realized without charge transport loss. Further studies are required to establish clear guidelines for material and device design to achieve a high FF.

4. Conclusion

We described how the photovoltaic parameters of J_{SC}, V_{OC}, and FF can be understood from the viewpoint of photophysical elementary processes of photovoltaic conversion in

polymer solar cells. The photovoltaic conversion process is an ultrafast phenomenon that progresses over the wide time range from femtoseconds for light absorption to microseconds for charge collection: it is of the other of 10^9. Time-resolved spectroscopy using a short-pulse laser is an extremely effective observation technique for directly tracking these elementary processes in real time. Therefore, in this review, we described the analysis method of each characteristic parameter on the basis of some measurement examples. J_{SC} is obtained as the product of the efficiencies of each elementary process of light absorption, exciton diffusion, charge transfer, charge dissociation, and charge collection. Therefore, by evaluating the efficiency of each of these elementary processes, we can clarify which is a limiting process. The charge dissociation is particularly important in polymer solar cells, and previous studies have suggested that the high crystallinity and aggregates of the constituent materials are important factors in highly efficient charge dissociation. Interestingly, the energy offset required for the charge dissociation may not be as large as previously assumed. This finding can lead to the reduction in V_{OC} loss, as it was believed that the decrease in V_{OC} was inevitable as a trade-off owing to the offset required for high charge dissociation. Specifically, in a system with a small energy offset, this trade-off could be greatly relaxed, so that the additional voltage loss owing to the CT absorption band is suppressed and the nonradiative loss is relatively reduced by borrowing the radiative transition intensity of the exciton band, resulting in much smaller voltage loss. In order to achieve high efficiency, charge dissociation should be efficient as well even for such a small energy offset. Therefore, it is of particular importance to elucidate the mechanism that enables highly efficient charge dissociation even under low energy offset conditions. As for the FF, the difference in FF can be discussed on the basis of the recombination kinetic parameters in transport-limiting devices. In most cases, charge transport is the rate-limiting process; however, recently, devices that can be explained by the Shockley diode model have been reported. Currently, the trial-and-error method is the main approach for achieving a high FF, but it is necessary to establish the design guidelines for materials development and device fabrication systematically. I hope that, by the time this paper is published, an efficiency of 20% will already have been achieved.

Acknowledgments

This study is based partly on collaborative research with Professor Osaka at the Graduate School of Advanced Science and Engineering, Hiroshima University. This study was partly supported by the Grants-in-Aid for Scientific Research (21H04692) and the JST MIRAI Program (JPMJMI20E2). I would like to express my sincere gratitude to Professor Osaka for his valuable advice on this draft.

References

[1] J. J. M. Halls, C. A. Walsh, N. C. Greenham, E. A. Marseglia, R. H. Friend, S. C. Moratti, and A. B. Holmes, Nature **376**, 498 (1995).
[2] G. Yu, J. Gao, J. C. Hummelen, F. Wudl, and A. J. Heeger, Science **270**, 1789 (1995).
[3] M. Hiramoto, H. Fujiwara, and M. Yokoyama, Appl. Phys. Lett. **58**, 1062 (1991).
[4] J. C. Hummelen, B. W. Knight, F. LePeq, and F. Wudl, J. Org. Chem. **60**, 532 (1995).
[5] F. Padinger, R. S. Rittberger, and N. S. Sariciftci, Adv. Funct. Mater. **13**, 85 (2003).
[6] Y. Liang, Z. Xu, J. Xia, S.-T. Tsai, Y. Wu, G. Li, C. Ray, and L. Yu, Adv. Mater. **22**, E135 (2010).
[7] Y. Lin, J. Wang, Z.-G. Zhang, H. Bai, Y. Li, D. Zhu, and X. Zhan, Adv. Mater. **27**, 1170 (2015).
[8] S. Honda, T. Nogami, H. Ohkita, H. Benten, and S. Ito, ACS Appl. Mater. Interfaces **1**, 804 (2009).
[9] L. Zhu, M. Zhang, J. Xu, C. Li, J. Yan, G. Zhou, W. Zhong, T. Hao, J. Song, X. Xue, Z. Zhou, R. Zeng, H. Zhu, C.-C. Chen, R. C. I. MacKenzie, Y. Zou, J. Nelson, Y. Zhang, Y. Sun, and F. Liu, Nat. Mater. **21**, 656 (2022).
[10] H. Ohkita and S. Ito, Polymer **52**, 4397 (2011).
[11] H. Ohkita and S. Ito, in *Organic Solar Cells*, ed. W. H. Choy (Springer, 2013).
[12] H. Ohkita, Y. Tamai, H. Benten, and S. Ito, IEEE J. Sel. Top. Quantum Electron. **22**, 100 (2016).
[13] H. Ohkita, in *Organic Solar Cells*, ed. M. Hiramoto and S. Izawa (Springer, 2020).
[14] J. Guo, H. Ohkita, H. Benten, and S. Ito, J. Am. Chem. Soc. **132**, 6154 (2010).
[15] K. Kawashima, Y. Tamai, H. Ohkita, I. Osaka, and K. Takimiya, Nat. Commun. **6**, 10085 (2015).
[16] D. Chen, A. Nakahara, D. Wei, D. Nordlund, and T. P. Russell, Nano Lett. **11**, 561 (2011).
[17] A. Salleo, R. J. Kline, D. M. DeLongchamp, and M. L. Chabinyc, Adv. Mater. **22**, 3812 (2010).
[18] D. E. Motaung, G. F. Malgas, and C. J. Arendse, J. Mater. Sci. **45**, 3276 (2010).
[19] K. Kawashima, T. Fukuhara, Y. Suda, Y. Suzuki, T. Koganezawa, H. Yoshida, H. Ohkita, I. Osaka, and K. Takimiya, J. Am. Chem. Soc. **138**, 10265 (2016).
[20] Y. Tamai, K. Tsuda, H. Ohkita, H. Benten, and S. Ito, Phys. Chem. Chem. Phys. **16**, 20338 (2014).
[21] H.-Y. Chen, J. Hou, A. E. Hayden, H. Yang, K. N. Houk, and Y. Yang, Adv. Mater. **22**, 371 (2010).
[22] A. A. Guilbert, J. M. Frost, T. Agostinelli, E. Pires, S. Lilliu, J. E. Macdonald, and J. Nelson, Chem. Mater. **26**, 1226 (2014).
[23] S. Yamamoto, H. Ohkita, H. Benten, and S. Ito, J. Phys. Chem. C **116**, 14804 (2012).
[24] S. Yamamoto, H. Ohkita, H. Benten, S. Ito, S. Yamamoto, D. Kitazawa, and J. Tsukamoto, J. Phys. Chem. C **117**, 10277 (2013).
[25] D. Veldman, Ö. İpek, S. C. J. Meskers, J. Sweelssen, M. M. Koetse, S. C. Veenstra, J. M. Kroon, S. S. van Bavel, J. Loos, and R. A. J. Janssen, J. Am. Chem. Soc. **130**, 7721 (2008).
[26] G. Grancini, M. Maiuri, D. Fazzi, A. Petrozza, H.-J. Egelhaaf, D. Brida, G. Cerullo, and G. Lanzani, Nat. Mater. **12**, 29 (2013).
[27] S. Gélinas, A. Rao, A. Kumar, S. L. Smith, A. W. Chin, J. Clark, T. S. van der Poll, G. C. Bazan, and R. H. Friend, Science **343**, 512 (2013).
[28] K. Vandewal, S. Albrecht, E. T. Hoke, Kenneth R. Graham, J. Widmer, J. D. Douglas, M. Schubert, W. R. Mateker, J. T. Bloking, G. F. Burkhard, A. Sellinger, J. M. J. Fréchet, A. Amassian, M. K. Riede, M. D. McGehee, D. Neher, and A. Salleo, Nat. Mater. **13**, 63 (2014).
[29] C. Deibel, T. Strobel, and V. Dyakonov, Phys. Rev. Lett. **103**, 036402 (2009).
[30] B. Bernardo, D. Cheyns, B. Verreet, R. D. Schaller, B. P. Rand, and N. C. Giebink, Nat. Commun. **5**, 3245 (2014).
[31] H. Ohkita, S. Cook, Y. Astuti, W. Duffy, S. Tierney, W. Zhang, M. Heeney, I. McCulloch, J. Nelson, D. D. C. Bradley, and J. R. Durrant, J. Am. Chem. Soc. **130**, 3030 (2008).
[32] B. A. Gregg, J. Phys. Chem. Lett. **2**, 3013 (2011).
[33] C. Groves, Energy Environ. Sci. **6**, 1546 (2013).
[34] T. M. Burke and M. D. McGehee, Adv. Mater. **26**, 1923 (2014).
[35] S. N. Hood and I. Kassal, J. Phys. Chem. Lett. **7**, 4495 (2016).
[36] W. Kaiser, V. Janković, N. Vukmirović, and A. Gagliardi, J. Phys. Chem. Lett. **12**, 6389 (2021).
[37] A. Markina, K.-H. Lin, W. Liu, C. Poelking, Y. Firdaus, D. R. Villalva, J. I. Khan, S. H. K. Paleti, G. T. Harrison, J. Gorenflot, W. Zhang, S. D. Wolf, I. McCulloch, T. D. Anthopoulos, D. Baran, F. Laquai, and D. Andrienko, Adv. Energy Mater. **11**, 2102363 (2021).
[38] N. C. Giebink, G. P. Wiederrecht, M. R. Wasielewski, and S. R. Forrest, Phys. Rev. B **83**, 195326 (2011).
[39] M. Gruber, J. Wagner, K. Klein, U. Hormann, A. Opitz, M. Stutzmann, and W. Brutting, Adv. Energy Mater. **2**, 1100 (2012).

[40] L. J. A. Koster, S. E. Shaheen, and J. C. Hummelen, Adv. Energy Mater. **2**, 1246 (2012).
[41] R. A. J. Janssen and J. Nelson, Adv. Mater. **25**, 1847 (2013).
[42] M. Saito, H. Ohkita, and I. Osaka, J. Mater. Chem. A **8**, 20213 (2020).
[43] J. Jean, T. S. Mahony, D. Bozyugit, M. Sponseller, J. Holovský, M. G. Bawendi, and V. Bulović, ACS Energy Lett. **2**, 2616 (2017).
[44] D. Qian, Z. Zheng, H. Yao, W. Tress, T. R. Hopper, S. Chen, S. Li, J. Liu, S. Chen, J. Zhang, X.-K. Liu, B. Gao, L. Ouyang, Y. Jin, G. Pozina, I. A. Buyanova, W. M. Chen, O. Inganäs, V. Coropceanu, J.-L. Bredas, H. Yan, J. Hou, F. Zhang, A. A. Bakulin, and F. Gao, Nat. Mater. **17**, 703 (2018).
[45] S. Liu, J. Yuan, W. Deng, M. Luo, Y. Xie, Q. Liang, Y. Zou, Z. He, H. Wu, and Y. Cao, Nat. Photonics **14**, 300 (2020).
[46] F. D. Eisner, M. Azzouzi, Z. Fei, X. Hou, T. D. Anthopoulos, T. J. S. Dennis, M. Heeney, and J. Nelson, J. Am. Chem. Soc. **141**, 6362 (2019).
[47] D. Bartesaghi, I. del C. Pérez, J. Kniepert, S. Roland, M. Turbiez, D. Neher, and L. J. A. Koster, Nat. Commun. **6**, 7083 (2015).
[48] D. Neher, J. Kniepert, A. Elimelech, and L. J. A. Koster, Sci. Rep. **6**, 24861 (2016).
[49] A. Maurano, C. G. Shuttle, R. Hamilton, A. M. Ballantyne, J. Nelson, W. Zhang, M. Heeney, and J. R. Durrant, J. Phys. Chem. C **115**, 5947 (2011).
[50] G. F. A. Dibb, F. C. Jamieson, A. Maurano, J. Nelson, and J. R. Durrant, J. Phys. Chem. Lett. **4**, 803 (2013).
[51] Y. Zeng, D. Li, Z. Xiao, H. Wu, Z. Chen, T. Hao, S. Xiong, Z. Ma, H. Zhu, L. Ding, and Q. Bao, Adv. Energy Mater. **11**, 2101338 (2021).

Profile

Hideo Ohkita obtained a Doctoral degree at Kyoto University in 1997. He became an Assistant Professor in 1997, promoted to Associate Professor in 2006, and to Professor in the Department of Polymer Chemistry at Kyoto University in 2016. His main research interests include studying photophysics and photochemistry in polymer systems. His current research focuses on spectroscopic and device physics approach to polymer solar cells.